This Project has received funding from the European Union's Horizon 2020 Research and Innovation Programme under Grant Agreement N. 884157

FLExibilize combined cycle power plant through power-to-X solutions using non-CONventional Fuels

D2.6 – "Evaluation of the Global impact of H2/NH2 based combustion processes"

Organization name of lead contractor: UCL

Project Contractual Details

Project Title	FLExibilize combined cycle power plant through power-to-X solutions using non-CONventional Fuels
Project Acronym	FLEXnCONFU
Grant Agreement No.	884157
Project Start Date	01-04-2020
Project End Date	31-03-2024
Duration	48 months
Website	www.flexnconfu.eu

Deliverables Details

Number	D2.6		
Title	**Evaluation of the Global impact of H2/Nh2 based combustion processes**		
Work Package	WP2		
Dissemination level[1]	PU		
Due date (M)	31/05/2023	Submission date (M)	04/04/2024
Deliverable responsible	Azd Zayoud (UCL)		
Contributing Author(s)	Azd Zayoud (UCL)		
Reviewer(s)	Julio Guillen (CIRCE), Antonio Campanale (RINA)		
Final review and quality approval	26/03/2024		

Document History

Date	Version	Name	Changes
21/09/2022	1.0	Azd Zayoud	First issue
30/12/2022	2.0	Azd Zayoud	revised
24/01/2023	3.0	Julio Guillen	revised
24/01/2023	4.0	Azd Zayoud	Final version for submission
04/04/2024	5.0	Antonio Campanale	Version reviewed for submission

[1] PU = Public

CO = Confidential, only for members of the consortium (including Commission Services)

Table of Contents

List of Figures

1 Introduction

The work has been prepared in the context of the Task 2.5 “Global impact of H2/NH3 based combustion processes” which is focused on evaluating the contribution of the imported synthetic renewables-based electro-fuel namely hydrogen and ammonia; and their usage in the energy sector. The two major objectives of the model are: 1. Minimisation of the economic cost (LCOH, LCOE); 2. Minimisation of the Global Warming Potential (GWP).

Note that in the WP1 the techno-economic analysis was performed for applied P2X2P concept in situ, where the locally produced power is stored in energy vectors, namely H2/NH3 and subsequently used to power CCGT for electricity generation. In the present task 2.5, the work has been focused on the imported green fuels; it provides partners involved in the FLEXnCONFU project a simulation tool for deterministic and robust design optimisation that can be used to assess the economic cost (LCOH, LCOE) and Global Warming Potential (GWP) (CO_2 emission intensity) of the imported green e-fuels. Furthermore, the simulation tool helps in optimising the system’s parts, such as PV panels capacity and types, electrolyser capacity… under a wide range of operating modes for different production locations. This provides the decision makers a handy tool to compare between several scenarios of green e-fuel (green e-fuel refers to the e-fuel that is produced using renewable energy) production in several regions.

PV panels were the primary source of electricity, however, additional renewable energy sources (e.g. wind energy) can be used and wind turbine sub-model can be integrated. To achieve these objectives, a Python framework, namely RHEIA is employed; RHEIA provides multi-objective optimisation (deterministic and stochastic) and uncertainty quantification algorithms. Non-dominated Sorting Genetic Algorithm (NSGA-II) is implemented for the optimisation process. Minimising the LCOH, LCOE and minimising GWP of CO2 are set as objectives.

Interestingly, the proposed concept by FLEXnCONFU project P2X2P can be applied to several systems and various configurations. In this work, two scenarios are proposed. In the first scenario, the green hydrogen is generated using solar energy and transported via pipelines, subsequently it can be used to produce ammonia to power combined-cycle gas turbine (CCGT) power plant for electricity production. In the second scenario, the CCGT is powered with a fuel mixture of 30% H_2 and 70% NH_3 which is synthesised in a Haber-Bosch plant with a green H_2. However, using either 100% NH_3 fuel or 30-70% H_2-NH_3 fuel mixture depends on the gas turbine operating characteristics and the final LCOE and GWP [1].

2 Task planning

Dependency on the published literature data, projection of hydrogen supply and demand across Europe in 2030 and 2040 [2, 3], the green H2 importing regions are defined. Meanwhile, the second step of defining the production and exporting of green hydrogen regions is conducted depending on:

1. The potential of solar irradiance and constraint's level 1 (excluding complex terrain, large water bodies, compact forests, uninhabited areas, Intra-urban areas) and 2 (excluding protected areas and cropland).
2. Energy return on investment (EROI).

The tasks in the WP1 are someway related to this task 2.5, in terms of X2P layouts and components optimisation (e.g. electrolyser capacity [MW], storage capacity [Kg], etc.), however, in the present task, besides deterministic optimisation, this task will include uncertainty quantification analysis; furthermore, the objectives are focused on imported green e-fuel. The developed models can be used to estimate the cost (LCOH, LCOE) and associated GWP of the imported e-fuels (hydrogen) from Europe neighbouring countries in middle east and north Africa (MENA) under uncertainty.

In the energy system models, we can define two types of variables: 1. system parameters, which are beyond of designer's control e.g., efficiencies of electrolyser and PV panel) 2. design variables, which are optimised through deterministic design optimisation methods. The system parameters can be uncertain (e.g. CAPEX of PEM electrolyser, CAPEX of PV, interest rate etc...). This parametric uncertainty can be considered in design optimisation as well, resulting in alternative designs.

In the present task, 3 major steps are planned:

- Optimising the renewable energy system for H_2 production depending on the production location, H2 production quantity with 2 objects: minimising LCOH and minimising carbon emission intensity (CI).
- Power to X to power (case 1): electricity production in Cologne using 100% NH_3 as fuel to power CCGT, with 2 objects: minimising LCOE and minimising carbon emission intensity (CI).
- Power to X to power (case 2): electricity production in Cologne using 30-70% H_2-NH_3 fuel mixture to power CCGT, with 2 objects: minimising LCOE and minimising carbon emission intensity (CI).

3 System Model:

In this task, the computational framework, namely RHEIA [4] is used to facilitate multi-objective optimisation of the engineering model and uncertainty quantifications. The framework is based on Python programming language and the engineering models. The well-established evolutionary algorithm Non-dominated Sorting Genetic Algorithm (NSGA-II) is used for the deterministic design optimisation process. The NSGA-II is used to optimise (maximise, minimise) the quantity of interest so called design variable. The optimisation method and coding are explained in the appendix (page, 29).

In this section, the energy system model is described in detail. The model of converting solar energy into electricity and hydrogen is described; and transporting green hydrogen from MENA is considered being via pipeline network, which is a combination of new pipelines and repurposed pipelines.

3.1 Power2X2Power system modelling

To convert the solar energy into electric power, a PV array is considered. A single PV cell is characterised based on a single diode model without parallel resistance, following the experimentally validated structure presented by González-Longatt [5]. The produced PV cell current IPV depends on the photocurrent I_L, the diode current I_o and the series resistance R_s:

$$I_{PV} = I_L - I_O \left[exp\left(\frac{q(U_{PV} + I_{PV} R_S)}{n_d K T_{amb}} \right) - 1 \right] \qquad \text{Eq. 1}$$

Where q, is the electron charge k is the Boltzmann constant and n_d the diode ideality factor. The Newton-Raphson numerical method is used for its fast convergence and accuracy to solve this non-linear equation for I_{PV}. The photocurrent I_L depends on the solar irradiance G and ambient temperature T_{amb}:

$$I_L = I_{SC}(T_{1,\mathrm{nom}}) \frac{G}{1000} + K_0 \left(T_{\mathrm{amb}} - T_1 \right) \qquad \text{Eq. 2}$$

The coefficient K_o depends on the corresponding short-circuit currents $\boldsymbol{I_{SC}}$ and; T_1 and T_2 reference temperatures and:

$$K_0 = \frac{I_{SC}(T_2) - I_{SC}(T_1)}{T_2 - T_1}$$ Eq. 3

The diode current ***I₀*** is represented according to the following equation (4) and $I_0(T_1)$ is given by (5):

$$I_0 = I_0(T_1)\left(\frac{T_{amb}}{T_1}\right)^{\frac{3}{n}} \exp\left(\frac{qU_q(T_1)}{nk\left(\frac{1}{T_{amb}} - \frac{1}{T_1}\right)}\right)$$ Eq. 4

$$I_0(T_1) = \frac{I_{SC}(T_1)}{\left(\exp\left(\frac{qU_{OC}(T_1)}{nkT_1}\right) - 1\right)}$$ Eq. 5

The series resistance represents the internal losses (6):

$$R_s = -\frac{dU}{dI_{U_{OC}}} - \frac{1}{X_U}$$ Eq. 6

Where the term dU/dI_{UOC} is equal to 1.15/2/$N_{PV,s}$, based on the Photovoltaic panel current-voltage characteristic provided by the manufacturer. X_U is given by:

$$X_U = I_0(T_1)\frac{q}{nkT_1}\exp\left(\frac{qU_{OC}(T_1)}{nkT_1}\right) - \frac{1}{X_U}$$ Eq. 7

The shunt resistance, which corresponds to the leakage current to the ground, is commonly neglected and therefore it is not considered in this work [4, 6-8].

3.2 Electrolyser stack

The proton exchange membrane (PEM) electrolyser is chosen to produce hydrogen from the intermittent electricity supply. The PEM has a fast response time of <1 sec and full operational flexibility [9]. The experimentally validated model by Garcia-Valverde et al. is adopted, and the applied PEM electrolyser's operating voltage (U_{elec}) is calculated:

$$\mathrm{U_{elec}} = \mathrm{U_{rev}} + \mathrm{U_{electrodes}} + \mathrm{U_{ohm}} \quad \text{Eq. 8}$$

Table 1 shows the electrolyser's parameters that are required for modelling procedure.

Table 1: The PV-electrolyser system model parameters

Parameter	Deterministic value
n_{elec}	8000 h [9]
G	hourly data for one year [10]
T_{amb}	hourly data for one year [10]
μ_{ISC}	0.065 A/K [11]
μ_{UOC}	0.08 V/K [11]
I_{SC}	3.8 A [11]
U_{OC}	21.1 V [11]
A_m	50 cm^2 [11]
t_m	0.0051 cm
η_F	99.5% [11]
U_{degr}	6μV/h [11]
T_{elec}	design parameter[11]
i_{lim}	2 A/cm_2 [11]

(U_{rev}) is the reversible potential, ($U_{electrodes}$) is the overpotential at the electrodes, and (U_{elec}) is the ohmic overpotential. The current (I_{stack}= N_p·I_{elec}) and voltage (U_{stack}=N_s·U_{elec}) of the electrolyser 's stack depend on the number of combined electrolyser in parallel (N_p) and series (N_s). The hydrogen production is a function of Faraday efficiency (η_F), several electrolyser s in series (Ns), and current (I_{stack}).

$$\dot{m}_{H_2} = \frac{N_s I_{stack}}{2000F} \eta_F \quad \text{Eq. 9}$$

Further details are explained extensively in the published work by Garcia-Valverde et al. and Coppitters et al. [5, 11].

3.3 Transporting: Pipeline network

A pipeline network is considered for H_2 transportation in this study due to two facts. Firstly there is already an existing natural gas pipeline network that can be retrofitted; secondly, establishing a new pipeline network between MENA and EU is technically visible [12]. There are several factors that affect the $LCOE_{trans}$ via pipelines such as the distance, operating pressure, depreciation period of compressors and pipelines, CAPEX and OPEX of compressors and pipelines which vary depending on the size (diameter: <700mm, 700-900mm, and >900mm). For instance, the CAPEX of a small pipeline (<700mm) is (1.5 M€/km) almost 53% of the large pipeline CAPEX (2.8 M€/km at D >900mm); but the final $LCOE_{trans.}$ for small pipelines [0.05-0.14 €/kg/1000km] and large pipelines are comparable to each other [0.058-0.16 €/kg/1000km]. interestingly, retrofitting the existing natural gas pipeline network would reduce the $LCOE_{trans.}$ by 55±10% compared to the newly installed pipelines. The average $LCOE_{trans.}$ for 1000 km is 0.14 €/kg and deviates ±0.088 €/kg between the worst and the best scenarios. The $LCOE_{trans}$ for 1000, 2000, 3000 and 4000 km is [0.05, 0.23], [0.10, 0.46], [0.16, 0.68] and [0.21, 0.91], consequently. Compared to H_2 transport via pipelines (48”), shipping H_2 via Liquid organic hydrogen carriers (LOHC) and ammonia vectors could be competitive for distances longer than 3300 and 4400 km, respectively [13]. In the work, all transporting scenarios go through on-shore land, mainly which justifies H_2 transport from MENA to EU via pipelines rather than shipping. However, the final transporting via pipeline depends heavily on 1. Operating percentage of the pipeline, 2. Size of the pipeline network, 3. the percentage of newly instructed pipelines and percentage of repurposed natural gas pipeline network. In the case of 48 inches pipelines, the $CAPEX_{pipeline}$ and $OPEX_{pipeline}$ fall in the range of [0.02-0.29€/kg/1000km] and [0.01-0.02 €/kg/1000km] and the $CAPEX_{compressor}$ and $OPEX_{compressor}$ fall in the range of [0.04-0.07€/kg/1000km] and [0.02-0.04 €/kg/1000km] respectively. Figure 1 shows, for instance, the levelized cost of new and repurposed pipelines (48-inch) operating at 100%, 75%, and 25% capacity [13].

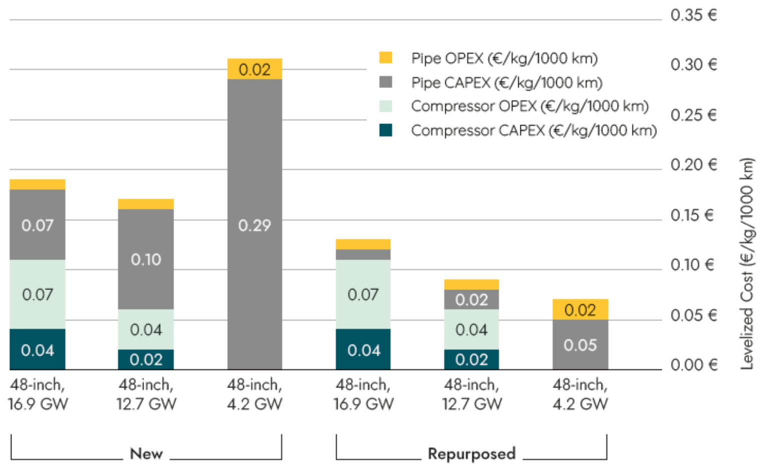

Figure 1 The levelized cost of new and repurposed pipelines 48" operating at 100%, 75%, and 25% capacity [13]

Concerning the CO_2 emissions, the indirect GHGs emission for gas transporting by pipelines has been adopted from published report, and in the worst and best cases the CO2 emissions are 0.18 and 0.11 kg.$CO_{2,eq}$/kg/1000km [14]. After converting the renewable energy into hydrogen and transporting via pipeline, ammonia is produced in Haber-Bosch plant to power CCGT.

3.4 Climate data

The climate [13] data, of hourly ground solar irradiance and ambient temperature, has been adapted to the studied hydrogen regions (e.g. Hassi R'mel, Algeria and Cologne, Germany, Figure 2). The data has been obtained via renewable[10]. The solar irradiance in Hassi R'mel, Algeria is ~40% higher than the one in Cologne, Germany. Additionally, the distribution of the solar irradiance is more uniform in Hassi R'mel compared to Cologne, which is desired for more stable operating conditions of the renewable energy system.

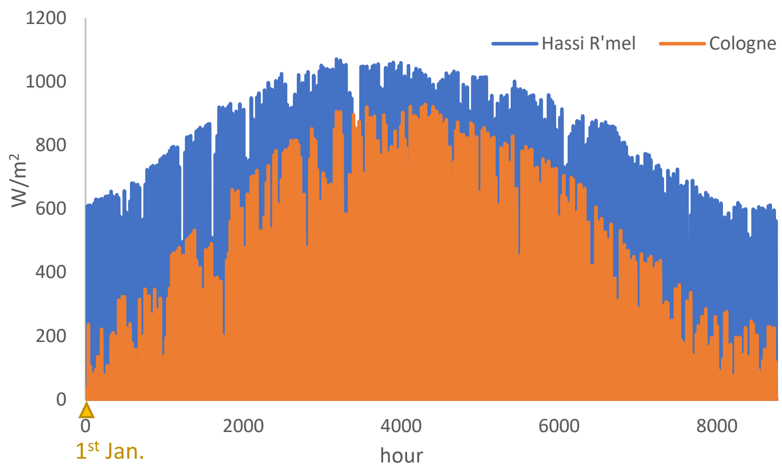

Figure 2 Hourly ground level solar irradiance in Hassi R'mel, Algeria and Cologne, Germany

3.5 Quantity of interest

An economic and environmental quantities of interest are defined to evaluate the system performance, namely levelized cost of energy (LCOE) and carbon intensity (CI). LCOE and CI correspond to the annualized system cost per unit of produced electricity and the annualized system green-house gases (GHG) namely CO_2 per unit of produced electricity.

$$LCOE = \frac{CAPEX_a + OPEX_a + C_{rep,a} + C_{grid,a}}{E} \qquad \text{Eq. 10}$$

The annualised capital expenses $CAPEX_a$ (13) and annualised operating expenses $OPEX_a$ (14) are scaled by the Capital Recovery Factor (CRF) and corresponds to the sum of the capital expenses for each component and the sum of the operating expenses [15]:

$$\mathrm{CAPEX_a} = \mathrm{CRF} \sum_{k=0}^{c} N_k \mathrm{CAPEX}_k \qquad \text{Eq. 11}$$

$$\mathrm{OPEX_a} = \sum_{k=0}^{c} N_k \mathrm{OPEX}_k \qquad \text{Eq. 12}$$

where c is the list of different components (i.e., DC–DC converters, PEM electrolyser array, PV array, compressor, storage tank, etc) and N corresponds to the installed capacity. The system lifetime L (25 years) and CRF is determined by the real interest rate i [15]:

$$\mathrm{CRF} = \frac{i(1+i)^L}{(1+i)^L - 1}$$ Eq. 13

where the real interest rate i considers the effect of inflation f on the nominal interest rate i':

$$i = \frac{i' - f}{1+f}$$ Eq. 14

The annualised replacement cost considers the costs related to the replacement of components during the system lifetime, where r_k is the number of replacements during the system lifetime for every component and t_k is the replacement period.:

$$C_{\mathrm{repl,a}} = \mathrm{CRF} \sum_{k=0}^{c} \left(N_k R_{\mathrm{c,k}} \sum_{l=0}^{r_k} (1+i)^{-l t_k} \right)$$ Eq. 15

Similar to the LCOE, the environmental quantity of interest represents the annualised GHG emission of the system per unit produced electricity (i.e., the CI):

$$CI = \frac{CAPEX_a + OPEX_a + C_{rep,a} + C_{grid,a}}{E}$$ Eq. 16

The annual GHG of the system per unit of produced electricity/e-fuel can be calculated similarly to the levelized cost of energy.

4 Case studies and results

The following sections present examples of a) Levelized cost of green hydrogen production and GWP in selected European regions and MENA regions. b) Levelized cost of electricity based on power to X to power (100% NH_3) case and GWP (CO_2 emission intensity) and c) Levelized cost of electricity based on power to X to power (30-70% H_2-NH_3) case and GWP (CO_2 emission intensity). In all cases, green electricity is produced via PV panels and used for hydrogen production.

4.1 Determining the consumption and production locations

The increased demand for renewable energy in a certain consumption region is not necessarily met with locally produced renewable energy; this requires importing energy from regions with high renewable energy potential.

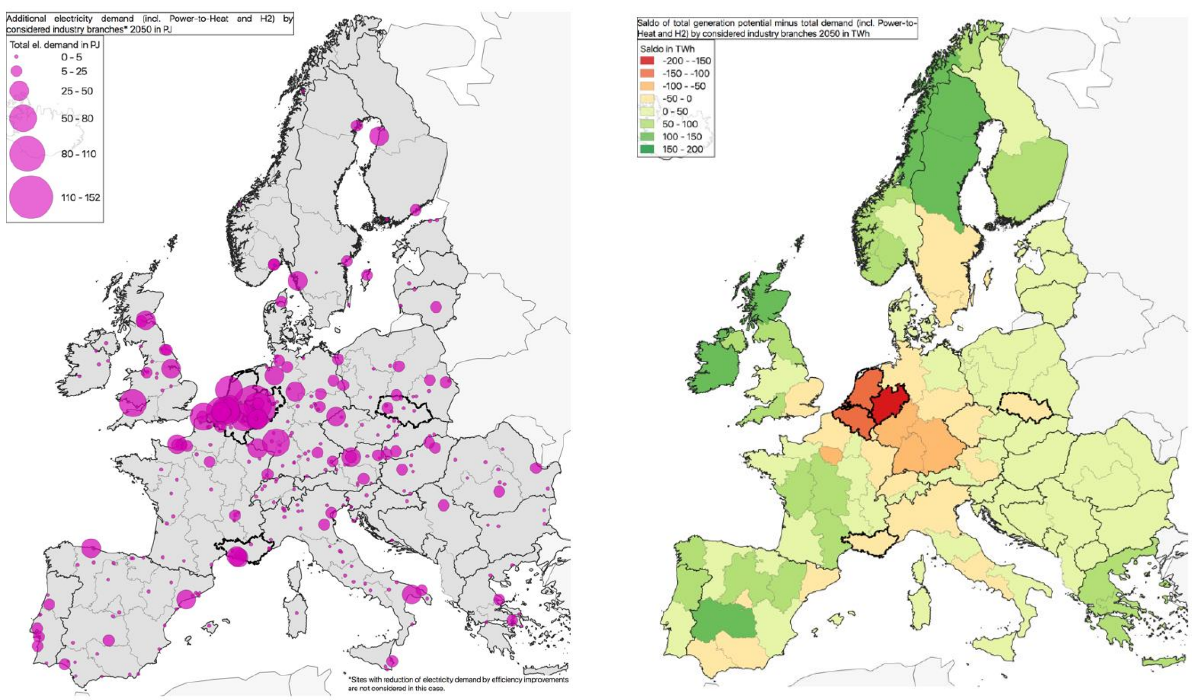

Figure 3 Left: regional distribution of the additional electricity demand (including Power-to-Heat and hydrogen) in PJ/a by decarbonised industry branches in 2050 ; right: regional distribution of difference between the potential electricity generation and total electricity demand in TWhe [16].

According to the Wuppertal Institute, the highest demand of electricity and hydrogen in Europe will be in north-west Europe. The power deficit is the highest in Benelux and North Rhine-Westphalia (Figure 3), which requires additional imported green H_2 to these locations. For the aforementioned reasons, in this task, Cologne is studied as an electricity production location using a green e-fuel (H_2-NH_3). In this power to X to [17] power scenario, two cases are studied based on the initial location of energy vector production (X); a. Local production of the H_2, b. H_2 production in MENA.

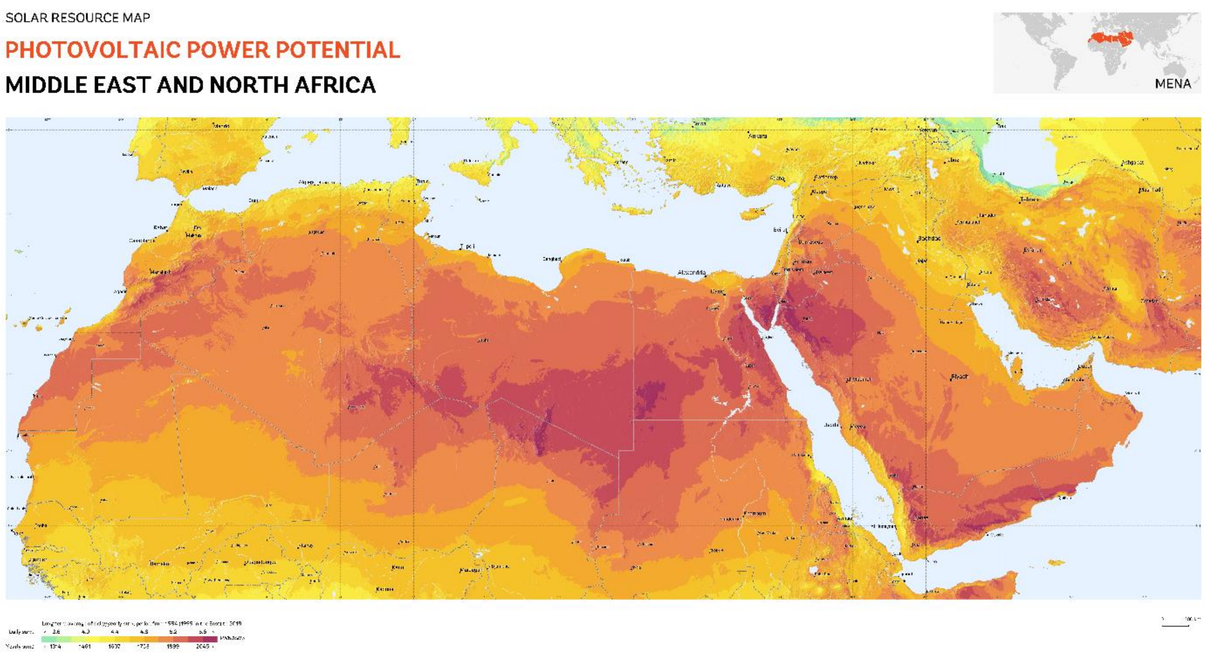

Figure 4 Photovoltaic power potential in Middle East and North Africa (MENA) [17, 18]

Three production locations are chosen in MENA namely Midelt, Morocco; Hassi R'mel, Algeria, Algeria and Sharma, Saudi due to high photovoltaic power potential (Figure 2) and higher stability of the solar irradiance over 8760 hour a year (Figure 4). Additionally, the natural gas pipeline network between Europe and MENA can be repurposed and new pipelines can be installed to transport green H2 from MENA to Europe.

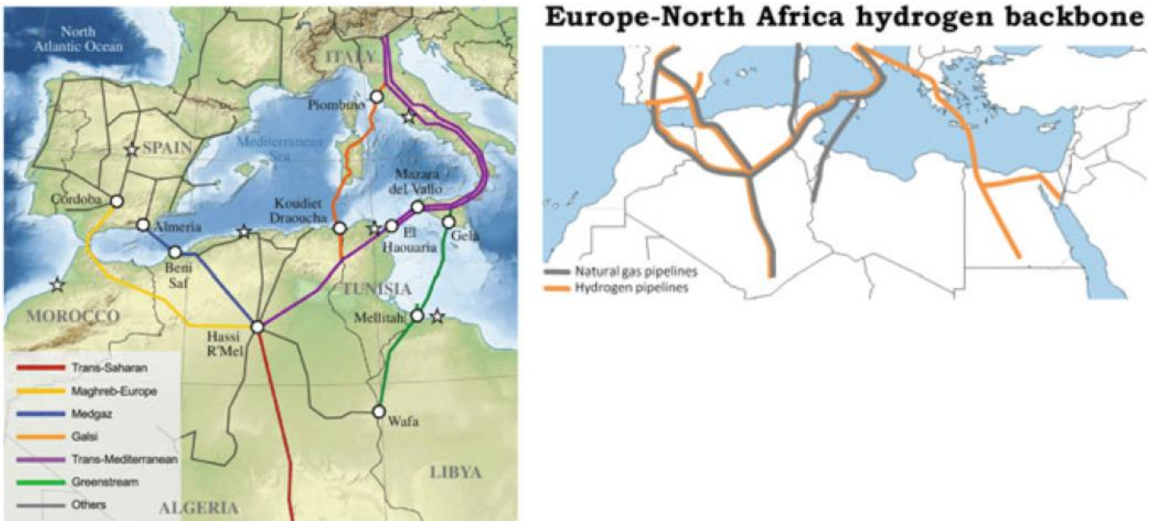

Figure 5 Natural gas infrastructure Europe–North Africa (left) and first outline for a hydrogen backbone infrastructure Europe–North Africa [19].

According to this scenario of transporting H_2 via pipeline networks, it has been assumed that transporting green energy is in the form of gaseous H_2 instead of shipping H_2 or NH_3. Subsequently, H_2 can be used directly or converted to NH_3.

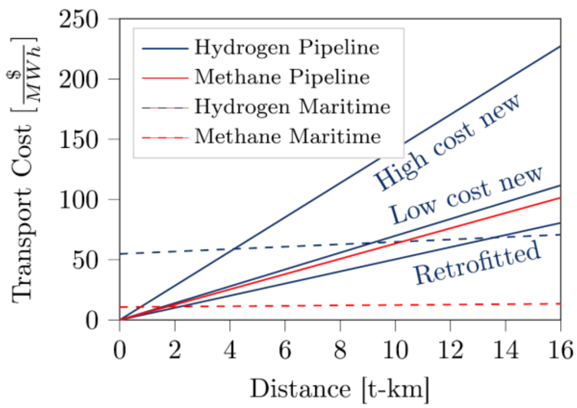

Figure 6 Transport costs of hydrogen and methane using existing infrastructure in the year 2030.

Figure 6 shows exemplary transport costs from Algeria to Germany assuming electricity costs of 40 and 45 $/MWh in the origin and destination countries [20].The cost of transporting H_2 via pipelines is cheapest in all cases for distances shorter than 4000 km.

4.2 PV-electrolyser optimisation for power to hydrogen production

Among the wide range of power to X storage methods, hydrogen is considered as a viable alternative as an energy vector [21]. The water electrolysis is one of the most robust and developed methods for hydrogen production. In this context of producing a green hydrogen, PV panels can be coupled to water electrolyser using DC-DC converters with tracking of Maximum PowerPoint (MPP). However, several design variables, e.g. PV capacity, electrolyser capacity, DC-DC etc., can be considered to perform multi-objective optimisation e.g. minimizing GWP (CO_2 intensity), maximizing H_2 production and minimizing LCOH.

Due to diversity in solar irradiance, temperature and operating conditions in H_2 production locations, renewable energy system optimisation becomes more important. Besides, performing deterministic optimisation analysis, the uncertainty analysis is considered as well to determine the parameters that contribute significantly to the objective variation, instead of depending on the unclearly defined modeller judgement. The determination of these individual contributions allows the formulation of environmental and economic guidelines to additional enhance the performance during real-life operations. The considered values for the different parameters are listed in Table 2

Table 2: Techno-economic considered parameters of the energy system

Parameter	min	max	average	unit	reference
CAPEXpv	350	600	475	€/kWp	[22]
OPEXpv	16	19	17.5	€/kWp/year	[23]
GHGpv	520	1550	1035	kgCO2,eq/kWe	[24]
CAPEXPEMEL2020	800	1200	1000	€/kW	[25]
CAPEXPEMEL2030	400	600	500	€/kW	[25]
OPEXPEMEL	3	5	4	% of CAPEX	[26]
repl. Costpemel	15	20	17.5	% of CAPEX	[27, 28]
lifetimepemel	60	100	80	kh	[25]
GHGPEMEL	190	235	212.5	kgCO2,eq/kW	[29]
CAPEXtank	11	14	12.5	€/kWh	[30]
OPEXtank	1	2	1.5	% of CAPEX	[31]
GHGtank	6	12	9	kgCO2,eq/kWh	[32]
CAPEXcompressor	1000	1500	1250	€/kW	[33]
OPEXcompressor	1	2	1.5	% of CAPEX	[33]
GHGcompressor	80	120	100	kgCO2,eq/kW	[34]
CAPEXDCDC	40	160	100	€/kW	[35]
OPEXDCDC	1	5	3	% of CAPEX	[35]
CAPEXpipeline	0.07	0.27	0.17	€/kg/1000 km	[13, 36]
OPEXpipeline	0.02	0.06	0.04	€/kg/1000 km	[13, 36]
CAPEXcompressor	0.02	0.04	0.03	€/kg/1000 km	[13, 36]
OPEXcompressor	0.05	0.07	0.06	€/kg/1000 km	[13, 36]
GHGpipeline	6.6	10.8	8.7	g.CO2/kg/1000 km	[14]

CAPEXCCGT	800	1200	1000	€/kW	[37-39]
OPEXCCGT,fixed	4	5	4.5	€/kW/year	[37, 38]
OPEXCCGT,variable			46	€/MWh	[37, 38]
lifetimeCCGT	25	35	30	year	[37, 38]
GHGCCGT	0			€/kW	[40]
CAPEXhb2	870		870	€/kW	[39]
OPEXhb	17		17	€/kW	[39]
GHGhb	0.024	0.04	0.032	kgCO2,eq/kg.NH3	[41]
CAPEX_NH3_tank	0.11	0.20	0.16	€/kWh	[42]
OPEX_NH3_tank	10	14	12	% OPEX	[42]
Interest r	2	6	4	%	[43]
inflation r	0	6	3	%	[44]

4.3 Green Hydrogen production LCOH and CO_2 intensity

The levelized cost of fuel and CO_2 intensity are crucial in the system performance assessment. The first step is decided to be focused on the green hydrogen production in Europe (case study, Cologne, Germany) and in 3 Europe neighbouring regions in MENA namely: Midelt, Morocco; Hassi R'mel, Algeria and Sharma, Saudi. The optimisation algorithm is applied to the system and considers average values of the system parameters (Table 1) and aimed at PEM electrolyser of 1.2 GW size; the average parameters of the system are considered, including the CAPEX of the electrolyser (1000 €/kW) in 2022. The required PV panel capacity is optimised and that results in Pareto front samples to minimise LCOH and minimise CO2 emission intensity.

For the four considered locations, the best minimal LCOH and CO2 emission intensity is in Sharma, Saudi; the LCOH is between 2.8 and 3.1 €/kg_{H2}, and the IC is between 1.4 and 1.3 $kg_{CO2,eq}/kg_{H2}$. Producing green hydrogen in Cologne, Germany has the worst scenario; the LCOE and CI are between 4.1 and 4.5 €/kg_{H2} (Figure 7); and 2.0 and 2.2 $kg_{CO2,eq}/kg_{H2}$. Interestingly, the LCOH is highly affected by the electrolyser CAPEX [4]. On one hand, the electrolyser CAPEX drops with the increased electrolyser capacity [25]. Reksten et al. projected the future cost of PEM and alkaline electrolysers which could drop from 1000 €/kW (in 2020) to 500 €/kW (in 2030). On the other hand, the hydrogen production is proportional to the total yearly solar irradiance,

[2] Including ASU.

which is the lowest in Cologne, Germany compared to the rest of cases, while the LCOH is inversely proportional to the total yearly solar irradiance.

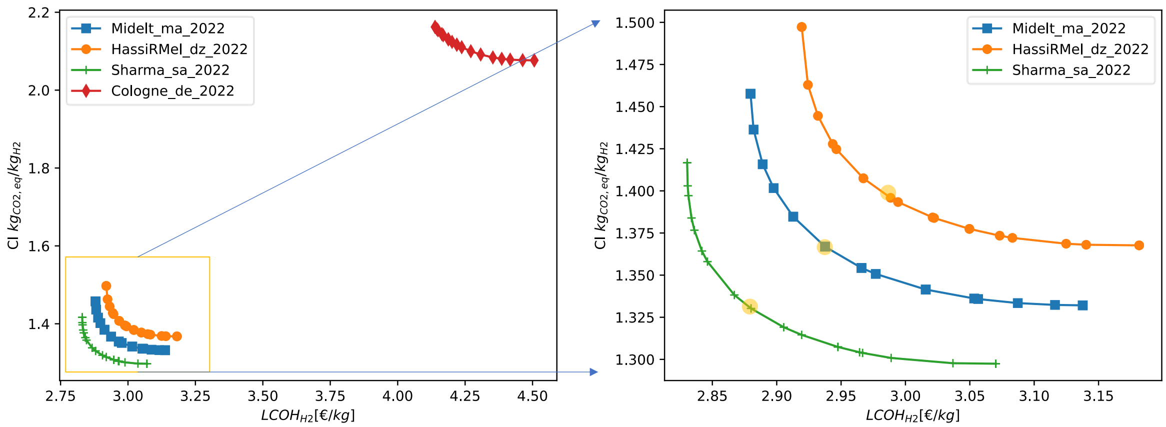

Figure 7 A trade-off exists between minimising CO2 intensity (CI) and minimising the Levelized Cost Of Hydrogen (LCOH) in 4 considered location. In the 3 locations in MENA, both of LCOH and CI are substantially lower compared to LCOH and CI in Cologne, Germany.

After getting the Pareto front (Figure 7), the knee points are defined to trade-off between LCOE and CI. A typical method to choose the most satisfactory design is to identify the knee point which corresponds to the design that gets the minimum Euclidian distance towards a utopia point (Figure 8). The knee-points of LCOH-CI Pareto front (in Sharma, Saudi, Midelt, Morocco; Hassi R'mel, Algeria; and in Cologne, Germany) give 2.90, 2.92, 2.96 and 4.23 €/kg_{H2}; and 1.34, 1.38, 1.40 and 2.11 $kg_{CO2,eq}/kg_{H2}$ consecutively.

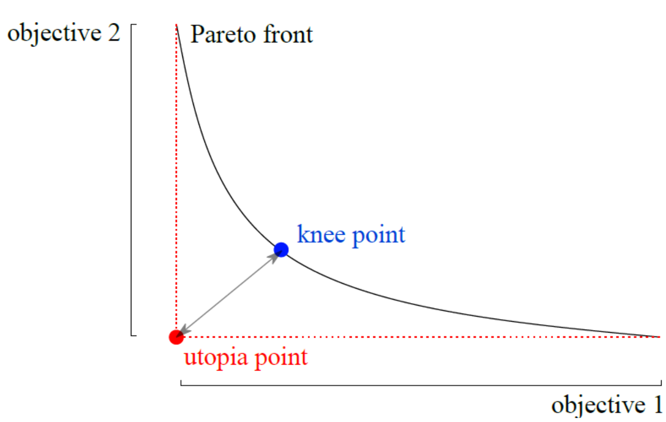

Figure 8 The knee point is the considered the optimal point on Pareto front that minimises LCOE and CI. The knee point has the minimal distance towards the utopia point. The utopia point is configured by the best values for both objectives [45].

In the design space of the system, the capacity of the electrolyser is set at 1.2 GW, and the PV capacity is treated as a design variable of the system and the PV capacity range is set between 1.2 to 2.1 GW. Interestingly, the same installed PV capacity (Figure 9, a) in MENA could reduce the CI by >0.5 $kg_{CO_2,eq}/kg_{H_2}$ compared to the same installed energy system in Cologne, Germany. The increased PV capacity from 1.3 to 2.0 GW can lead to higher H2 production, but it increases the CI by 0.2 $kg_{CO_2,eq}/kg_{H_2}$. However, the optimisation objectives of the work are focused on minimizing LCOH and minimizing CI (CO_2) emissions.

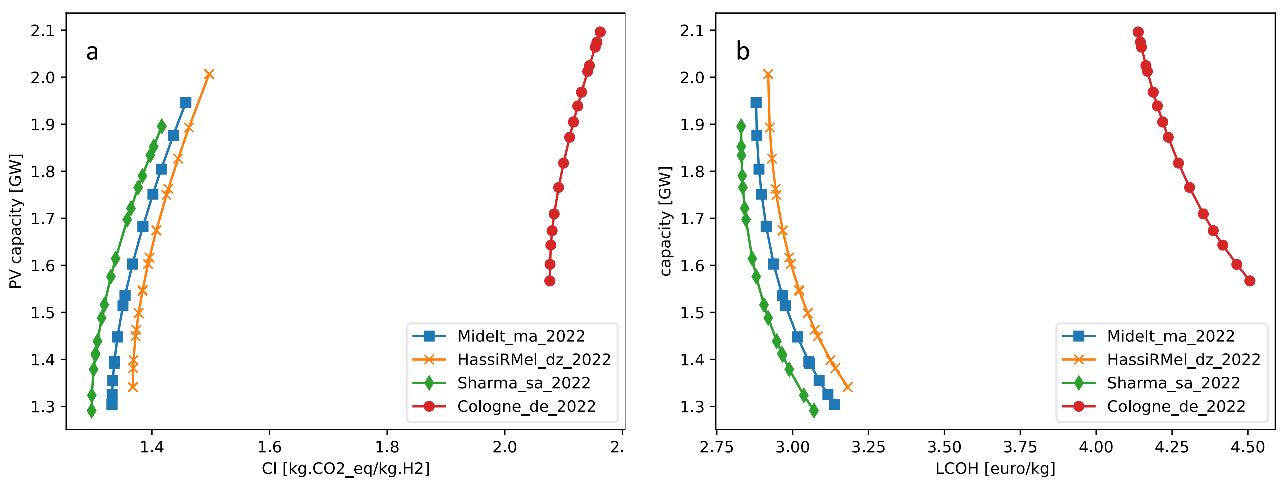

Figure 9 The optimisation objectives LCOH and CI (CO2) relationships with the design variable PV capacity in Europe neighbouring regions in MENA namely: Midelt, Morocco; Hassi R'mel, Algeria and Sharma, Saudi; and in Cologne, Germany.

Additionally, the LCOH of H_2 production in MENA is ~1.5 €/kg less than the LCOH of Cologne, Germany, for the same installed PV capacity. This is attributed mainly to the higher solar irradiance, which is ~40% higher in Midelt, Morocco, Hassi R'mel, Algeria and Sharma, Saudi compared to Cologne, Germany.

4.3.1.1 Uncertainty quantification of the CO2 emission intensity and LCOH

To quantify the uncertainty, Sobol' index is used to quantify the importance of a particular variable or factors in the variability of a system. It is commonly used in sensitivity analysis to identify the variables that have the greatest impact on the output of a model. The Sobol' indices can be used to analyse the 20 samples generated to determine the polynomial order 1, 2 or 3. Then, the worst-case (Leave-one-out error) LOO error is determined for the 20 design samples.

For CO2 intensity (CI) case, the polynomial of 1st order results in a LOO error of 6.3e-05 which is small enough to consider 1st order polynomial for CO2 intensity (CI) uncertainty quantification case. On the other hand, the increasing polynomial order from 1 to 2 and generating the PCE for the same design samples of LCOH decreases the worst-case LOO error from 0.0701 to 0.0140; as a result, the 2nd order polynomial is considered for the LCOH cases.

Regarding Sobol's indices, the number of uncertainty parameters can be reduced to 1 (co2_pv) which has 0.99 index; however, co2_pemel is considered as well which has the second Sobol's index. For LCOH quantification, out of the 12 uncertain parameters, 3 have a maximum Sobol' index below this threshold (*capex_pemel*, *int_rate*, *capex_pv*), meaning that they can be treated as deterministic without significantly affecting the calculated statistical moments of the LCOH.

Figure 10 The LCOH_2022 [€/kg] and CI [kg.CO2_eq/kg.H2] under uncertainty of capex_pemel, capex_pv, int_rate, co2pv and co2_pemel in Midelt, Morocco; Hassi R'mel, Algeria and Sharma, Saudi; and in Cologne, Germany

The uncertainty of CAPEX_pemel, int_rate, CAPEX_pv can lead to high LCOH variation. However, the LCOH in production location in MENA (Midelt, Morocco; Hassi R'mel, Algeria and Sharma, Saudi) has lower mean and deviation compared with the LCOH in Cologne, Germany

(Figure 10, a). the range span of LCOH is ~1.70 [€/kg] in MENA production locations compared to 2.54 [€/kg] in Cologne, Germany. On one hand, the optimistic values of CAPEX_pemel (800[€/kW]), int_rate (0.02), CAPEX_pv (350[€/kW]) leads to LCOH of 2.16, 2.20, 2.11 and 3.24 [€/kg] in Midelt, Morocco; Hassi R'mel, Algeria and Sharma, Saudi; and in Cologne, Germany. On the other hand, the pessimistic values of CAPEX_pemel (1200[€/kW]), int_rate (0.06), CAPEX_pv (600[€/kW]) leads LCOH of 3.86, 3.93, 378 and 5.78 [€/kg] in Midelt, Hassi R'mel and Sharma, and Cologne. The higher LCOH in Cologne is attributed to the lower solar irradiance and higher variation compared to H2 production locations in MENA (Figure 2), and the uncertainty of system parameters (CAPEX_pemel, int_rate, CAPEX_pv). For instance, the CAPEX is highly affected by the size of the electrolyser, this uncertain CAPEX may lead to significant variation in LCOH [25].

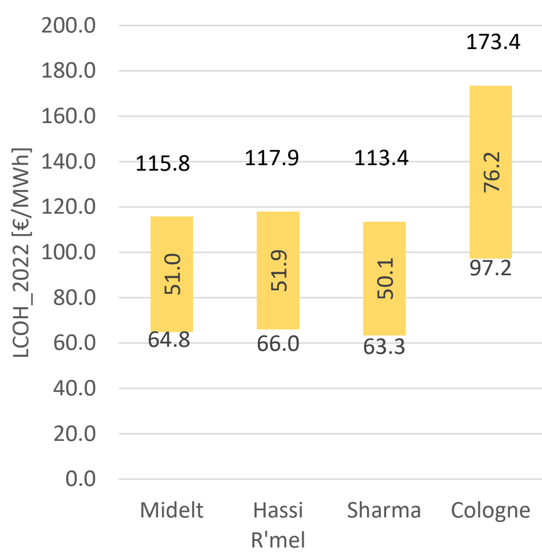

Figure 11 The LCOH_2022 in [€/MWh] under uncertainty of capex_pemel, capex_pv, int_rate, co2pv and co2_pemel in Midelt, Morocco; Hassi R'mel, Algeria and Sharma, Saudi; and in Cologne, Germany

Figure 11 represents the LCOH in [€/MWh]; the LCOHs in three MENA locations are similar to each other ± 4 [€/MWh] and fall in the range from 63.3 to 117.9 [€/MWh]. In Cologne, the LCOH is 35 to 60 [€/MWh] higher compared to other three locations' LCOHs; this variation is attributed to the lower solar irradiance and higher fluctuation in Cologne compared to MENA locations.

When it comes to the CI of H_2 production, CI is lower in MENA production locations and falls in a range of 0.30–0.43 [$kg_{CO_2,eq}/kg_{H_2}$] (Figure 10, b). Meanwhile, the CI in Cologne is between 0.46

and 0.63 $kg_{CO_2,eq}/kg_{H_2}$, these results are comparable to the achieved results by Simons and Bauer [46]. The GHG construction emissions of the PV and PEM electrolyser significantly affect the CI [24, 29]. However, green H2 production has remarkably a lower CI compared to the global CCO2 emission intensity (CI) of H2 production, which is between 10 and 20 [$kg_{CO_2,eq}/kg_{H_2}$] [46]. The lower GHG footprint of green H2 would give an additional economic value with applying carbon taxation [47]. The carbon tax in Europe differs widely from country to another country, e.g. the carbon tax in Poland is around 0.07 €/$ton_{CO_2,eq.}$ compared to 112 €/$ton_{CO_2,eq.}$ in Sweden [48].

4.3.1.2 Projection of LCOH in 2030

LCOH depends highly on the CAPEX_pemel and CAPEX_pv which are being reduced continuously due to scaling up and developed technologies; the average CAPEX_pv is expected to drop by 30% by 2030 compared to 2022 (475 €/kWp) [49]. On average, CAPEX_pemel is expected to reach ~500 €/kW in 2030 compared to ~1000 €/kW in 2022.

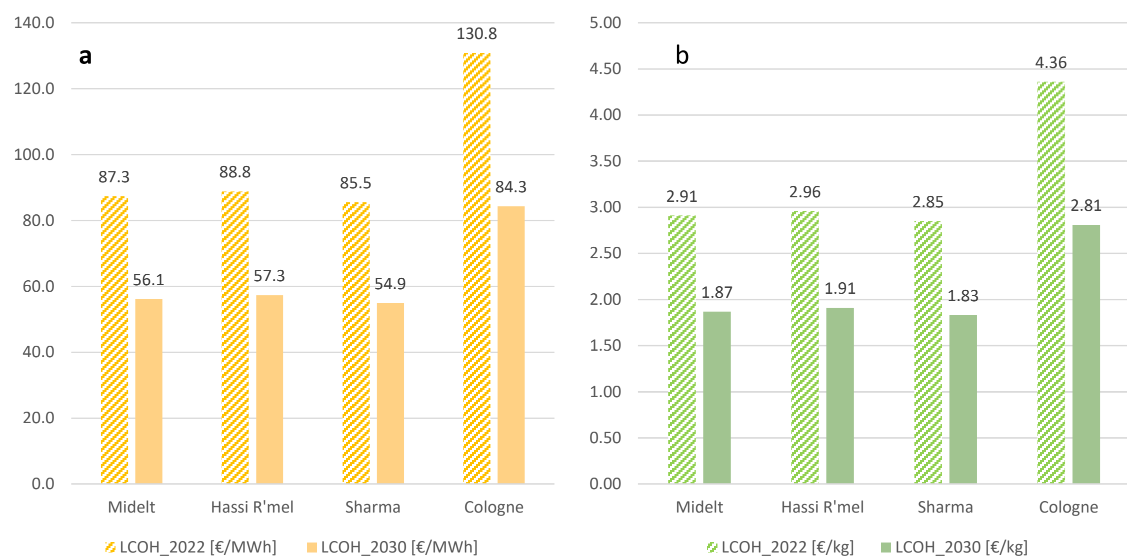

Figure 12 LCOH in 2022 versus LCOH projection in 2030 [€/kg] in Midelt, Morocco; Hassi R'mel, Algeria and Sharma, Saudi; and in Cologne, Germany

LCOH would drop sharply by 2030 compared to 2022, LCOH in MENA would fall below 2.0 [€/kg] threshold, which corresponds to 60 [€/MW] (Figure 12). However, the LCOH in Cologne would remain 1 [€/kg] more expensive compared to MENA selected production locations (Midelt, Morocco; Hassi R'mel, Algeria and Sharma, Saudi).

4.4 Power to X to Power case

The power to X to power model consists of sub-models for PV panels, DC/DC converter, PEM electrolyser, transporting hydrogen via pipelines (pipelines and compressors), storage, Haber-Bosch process, CCGT. The system parameters are described in Table 2. The CCGT is assumed to be 95 MWe. The sizes of PV, PEM, Haber-Bosch are optimised. The cost of hydrogen transportation via pipelines is studied. Both of LCOE and CO2 emission intensity (CI) have been minimised. In the following two cases are evaluated: 1. Power to X to power: 30-70% H_2-NH_3 fuel mixture for powering CCGT. Power to X to power: 100% NH_3 fuel mixture for powering CCGT.

4.4.1 Power to X to Power: 100% NH_3 fuel mixture for powering CCGT

The first case of power to X to power considers powering CCGT (95 MWe) with 100% NH3 fuel input. The fuel (100% NH3) is synthesised using the green hydrogen which produced locally or imported from MENA production locations.

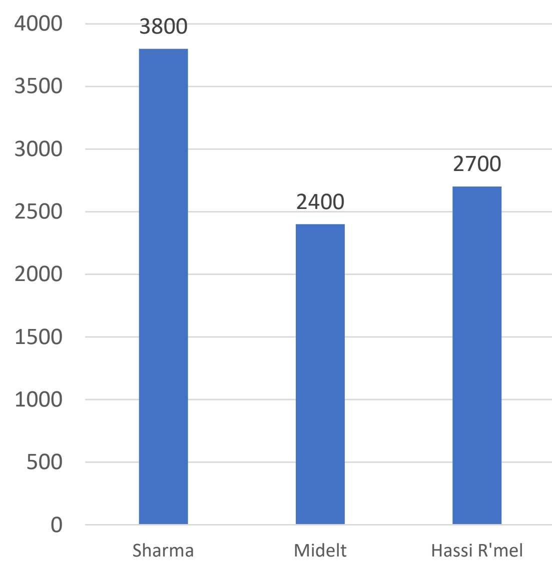

Figure 13 distance of transporting green hydrogen from MENA production locations to Cologne

Figure 13 shows the length of pipelines to transport hydrogen from MENA production locations to Cologne. As it is shown, the shortest distance to Cologne is 2400 km from Midelt compared to 2700 and 3800 km from Hassi R'mel and Sharma. The final transportation cost depends on the percentage of repurposed pipeline network and percentage of newly build pipelines. However, according to European Hydrogen Backbone, the pipeline CAPEX could be in the range of 0.07 to 0.27 €/kg/1000 km. Considering the average values of CAPEX and OPEX, the levelized cost of electricity based on green e-fuel (NH3) is shown in Figure 14.

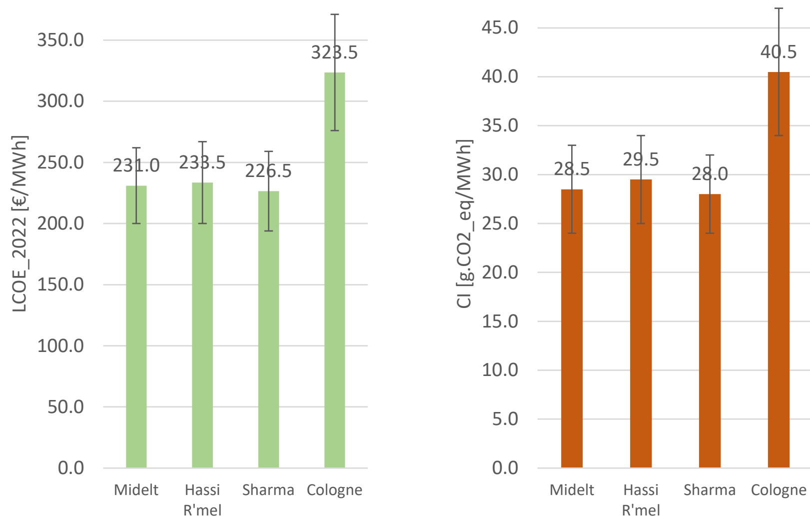

Figure 14 LCOE [€/MWh] and CI [g.CO_2_eq/kWh] of produced electricity in Cologne based on the production location of the green e-fuel used to power CCGT: 100% NH_3 fuel case

The average LCOE exceeds 200 €/MWh in all cases. Electricity production in Cologne using imported green e-fuel (100% NH_3) results in LCOEs of 231.0±21, 233.5±33.5 and 225.5±32.5 €/MWh for importing e-fuel cases from production locations namely Midelt, Hassi R'mel and Sharma. Even though the distance between Cologne and Sharma is the longest and the transportation cost is higher however, the lower LCOH compensates the higher transportation of H_2 via pipelines. And results in slightly lower LCOE. Powering the CCGT with locally produced green NH_3 results in a higher LCOE (323.5±47. 5 €/MWh) compared to electricity production using imported e-fuel from MENA production location; this higher LCOE is attributed to the higher cost of green H_2 production, which depends on the solar irradiance at the end. Besides the higher LCOE of produced electricity using locally produced e-fuel, the deviation of the LCOE is higher compared to the cases where H_2 is produced and imported from Midelt, Hassi R'mel and Sharma, due to higher uncertainty of solar irradiance Cologne.

The LCOE based on pure green e-fuel is lower than the average monthly electricity prices in Europe, which has been affected heavily by the global energy crises [50]. Based on Lazerd's Levelized Cost of Energy report, the LCOE of natural gas powered CCGT can exceed 250 [€/MWh] which has reached an unprecedented level in 2022 [50, 51]. In this scene, the EU energy mix needs to be diversified and a higher ration of renewable energy is required to decarbonise EU energy system. Interestingly, the CO_2 emission intensity (CI) of electricity production based on green renewable e-fuel has lower extremely footprint compared to the natural gas powered CCGT. Figure 14 shows the CI of electricity production in Cologne using imported green hydrogen and locally produced green hydrogen; for imported e-fuel from Midelt, Hassi R'mel and Sharma via pipelines the carbon emission intensity of electricity production reaches 28±4.5 [g.CO2_eq/kWh] which is lower than the CI for electricity production based on locally produced e-fuel in Cologne which hits a level of 40.5±6.5 [g.CO2_eq/kWh].

4.4.1 Power to X to Power: 30-70% H2-NH_3 fuel mixture for powering CCGT

In the second scenario, CCGT is powered with 30-70% H2-NH3 fuel mixture. The fuel mixture contains 70% NH3 which is synthesised using green H2 and 30% H2 which is produced using PEM electrolyser, transported, stored and used as a fuel with being converted to NH3.

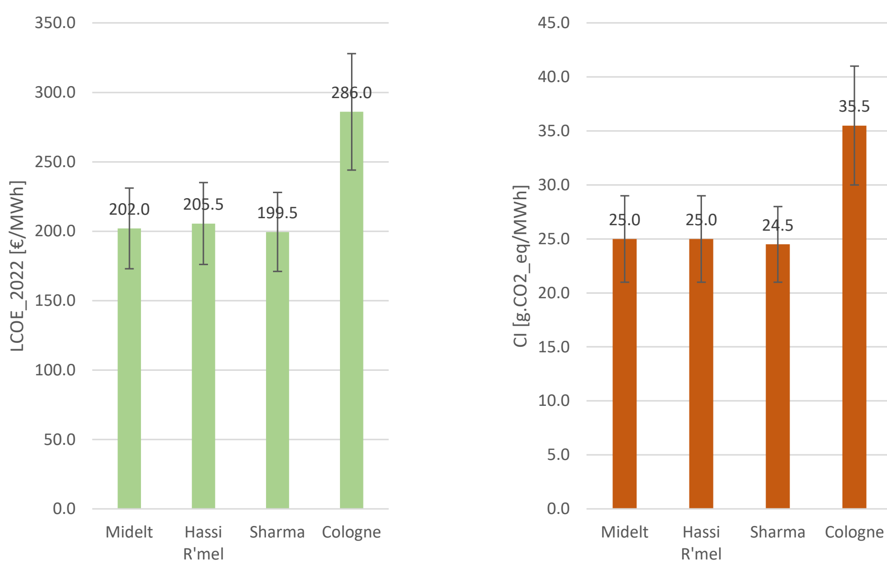

Figure 15 LCOE [€/MWh] and CI [g.CO2_eq/kWh] of produced electricity in Cologne based on the production location of the green e-fuel used to power CCGT: 30-70% H2-NH3 fuel mixture case

The electricity production based on 30-70% H2-NH3 fuel mixture case leads to ~12% lower LCOE compared to 100% NH3 case (Figure 15). The LCOEs drop from 231.0±21, 233.5±33.5 and 225.5±32.5 €/MWh (100% NH3 case) to 202.0±29, 205.5±29.5 and 199.5±28.5 €/MWh (100% NH3 case) for importing e-fuel from MENA production locations namely Midelt, Hassi R'mel and Sharma. Similarly, to electricity production based on 100% NH3 fuel case, the LCOE in Cologne based on locally produced e-fuel is higher than the produced electricity based on the imported e-fuel from MENA. Additionally, the carbon emission intensity (CI) is ~13.1% lower in the case of electricity production in Cologne based on 30-70% H2-NH3 case compared to 100% NH3 fuel case. Increasing the percentage of H2 in the H2-NH3 fuel mixture can lead to lower Ci as well as LCOE, but it will depend finally on the gas turbine operating conditions and the ability to run using a fuel mixture with higher H2 percentage; as well as the cost of storing H2 and NH3.

5 Conclusions

In the D2.6 the evaluation of global impact of the H_2-NH_3 is performed using the developed model in D2.3. The objectives of the task were focused on evaluating the contribution of the imported synthetic renewable based electro-fuel namely hydrogen and ammonia; and their usage in the energy sector. The two major objectives of the model are:

1. Minimisation of the economic cost (LCOH, LCOE)
2. Minimisation of the Global Warming Potential (GWP).

In WP1, T1.3 the techno-economic models were focused on the power to x to power scenarios that take in account the locally produced e-fuel (H_2 and NH_3). In the WP2, task 2.5 the models are focused on evaluating the rule of imported green e-fuel.

The deliverable D2.6 consists on a report in which the models developed are described. The description includes the models and the open source Python framework, which is used for optimisation. The model is used to optimise the capacity of the PV panel size and the PEM electrolyser size with objectives to minimise the carbon emission intensity and the levelized cost of H_2 and electricity. The procedure of performing the deterministic optimisation and uncertainty quantifications are described as well.

The results of the optimisation analysis shows that electricity production in EU power plants using pure green e-fuel has lower levelized cost of electricity LCOE and lower carbon emission intensity (CI) for imported green hydrogen from MENA compared to locally produced hydrogen case. Never the less, the carbon emission intensity (CI) of electricity production using imported or locally produced hydrogen is over 10 folds lower than the CI of electricity production using fossil fuel. The model is applied for electricity production in Cologne, Germany; which can be performed for other location in Europe.

The imported green e-fuel from EU neighbouring countries is technically visible, and economically viable. Additionally, it can secure the energy supply by diversifying the EU energy sources instead of relying heavily on unsecured energy sources.

Bibliography

[1] S. Patel, "Mitsubishi Power developing 100% ammonia-capable gas turbine," ed: Mar, 2021.

[2] ehb, "Five hydrogen supply corridors for Europe in 2030," 2022. [Online]. Available: https://ehb.eu/files/downloads/EHB-Supply-corridor-presentation-Full-version.pdf

[3] ehb, "EHB: A European hydrogen infrastructure vision covering 28 countries," 2022. [Online]. Available: https://gasforclimate2050.eu/wp-content/uploads/2022/04/EHB-A-European-hydrogen-infrastructure-vision-covering-28-countries.pdf.

[4] D. Coppitters. "Robust design optimization of renewable Hydrogen and dErIved energy cArrier systems (RHEIA)." https://rheia.readthedocs.io/en/latest/ (accessed.

[5] R. García-Valverde, N. Espinosa, and A. Urbina, "Optimized method for photovoltaic-water electrolyser direct coupling," *International Journal of Hydrogen Energy*, vol. 36, no. 17, pp. 10574-10586, 2011, doi: 10.1016/j.ijhydene.2011.05.179.

[6] F. M. González-Longatt, "Model of photovoltaic module in Matlab," *Ii Cibelec*, vol. 2005, pp. 1-5, 2005.

[7] Q. Kou, S. A. Klein, and W. A. Beckman, "A method for estimating the long-term performance of direct-coupled PV pumping systems," *Solar Energy*, vol. 64, no. 1-3, pp. 33-40, 1998, doi: 10.1016/s0038-092x(98)00049-8.

[8] D. Coppitters, K. Verleysen, W. De Paepe, and F. Contino, "How can renewable hydrogen compete with diesel in public transport? Robust design optimization of a hydrogen refueling station under techno-economic and environmental uncertainty," *Appl Energ*, vol. 312, 2022, doi: 10.1016/j.apenergy.2022.118694.

[9] A. Buttler and H. Spliethoff, "Current status of water electrolysis for energy storage, grid balancing and sector coupling via power-to-gas and power-to-liquids: A review," *Renewable and Sustainable Energy Reviews*, vol. 82, pp. 2440-2454, 2018, doi: 10.1016/j.rser.2017.09.003.

[10] S. Pfenninger and Iain Staffell. *renewables ninja*. [Online]. Available: https://www.renewables.ninja/

[11] D. Coppitters, W. De Paepe, and F. Contino, "Surrogate-assisted robust design optimization and global sensitivity analysis of a directly coupled photovoltaic-electrolyser system under techno-economic uncertainty," *Appl Energ*, vol. 248, pp. 310-320, 2019, doi: 10.1016/j.apenergy.2019.04.101.

[12] J. Jens, A. Wang, K. v. d. Leun, D. Peters, and M. Buseman, "Extending the European Hydrogen Backbone: A EUROPEAN HYDROGEN INFRASTRUCTURE VISION COVERING 21 COUNTRIES," 2021, vol. 3. [Online]. Available: https://gasforclimate2050.eu/wp-content/uploads/2021/06/European-Hydrogen-Backbone_April-2021_V3.pdf

[13] A. Wang *et al.*, "Analysing future demand, supply, and transport of hydrogen," 2021. [Online]. Available: https://gasforclimate2050.eu/wp-content/uploads/2021/06/EHB_Analysing-the-future-demand-supply-and-transport-of-hydrogen_June-2021_v3.pdf
[14] H. P. H. v. Essen, H. J. H. Croezen, and J. B. J. Nielsen, "Emission of pipeline transport compered with those of competing models

Environmental analysis of ethylene and propylene transport within the EU," 2003. [Online]. Available: www.ce.nl
[15] B. Zakeri and S. Syri, "Electrical energy storage systems: A comparative life cycle cost analysis," *Renewable and Sustainable Energy Reviews*, vol. 42, pp. 569-596, 2015/02/01/ 2015, doi: https://doi.org/10.1016/j.rser.2014.10.011.
[16] F. Merten, A. Nebel, C. Krüger, C. Schneider, A. Scholz, and A. Taubitz, "Needs of electricity, hydrogen and carbon infrastructures for greenhouse gas neutral heavy industry clusters in the EU 2050," 2020: European Council for an Energy Efficient Economy.
[17] ESMAP, "Global Photovoltaic Power Potential by Country," 2020.
[18] ESMAP. *Global Solar Atlas 2.0, a free, web-based application is developed and operated by the company Solargis s.r.o. on behalf of the World Bank Group, utilizing Solargis data, with funding provided by the Energy Sector Management Assistance Program (ESMAP)*. [Online]. Available: https://globalsolaratlas.info
[19] A. van Wijk and F. Wouters, "Hydrogen–The Bridge Between Africa and Europe," in *Shaping an Inclusive Energy Transition*, 2021, ch. Chapter 5, pp. 91-119.
[20] M. Moritz, M. Schönfisch, and S. Schulte, "Estimating global production and supply costs for green hydrogen and hydrogen-based green energy commodities," *International Journal of Hydrogen Energy*, 2022, doi: 10.1016/j.ijhydene.2022.12.046.
[21] M. Aneke and M. Wang, "Energy storage technologies and real life applications – A state of the art review," *Appl Energ*, vol. 179, pp. 350-377, 2016, doi: 10.1016/j.apenergy.2016.06.097.
[22] Franunhofer, "Photovoltaics Report," 2022. [Online]. Available: https://www.ise.fraunhofer.de/content/dam/ise/de/documents/publications/studies/Photovoltaics-Report.pdf
[23] L. Reichenberg, F. Hedenus, M. Odenberger, and F. Johnsson, "The marginal system LCOE of variable renewables – Evaluating high penetration levels of wind and solar in Europe," *Energy*, vol. 152, pp. 914-924, 2018, doi: 10.1016/j.energy.2018.02.061.
[24] T. F. Kristjansdottir, C. S. Good, M. R. Inman, R. D. Schlanbusch, and I. Andresen, "Embodied greenhouse gas emissions from PV systems in Norwegian residential Zero Emission Pilot Buildings," *Solar Energy*, vol. 133, pp. 155-171, 2016.
[25] A. H. Reksten, M. S. Thomassen, S. Møller-Holst, and K. Sundseth, "Projecting the future cost of PEM and alkaline water electrolysers; a CAPEX model including electrolyser plant size and technology development," *International Journal of Hydrogen Energy*, vol. 47, no. 90, pp. 38106-38113, 2022, doi: 10.1016/j.ijhydene.2022.08.306.

[26] S. A. Grigoriev, V. N. Fateev, D. G. Bessarabov, and P. Millet, "Current status, research trends, and challenges in water electrolysis science and technology," *International Journal of Hydrogen Energy*, vol. 45, no. 49, pp. 26036-26058, 2020, doi: 10.1016/j.ijhydene.2020.03.109.
[27] B. Guinot *et al.*, "Techno-economic study of a PV-hydrogen-battery hybrid system for off-grid power supply: Impact of performances' ageing on optimal system sizing and competitiveness," *International journal of hydrogen energy*, vol. 40, no. 1, pp. 623-632, 2015.
[28] W. G. Colella, B. D. James, J. M. Moton, G. Saur, and T. Ramsden, "Techno-economic analysis of PEM electrolysis for hydrogen production," in *Electrolytic hydrogen production workshop, NREL, Golden, Colorado*, 2014, vol. 27.
[29] X. Zhang, C. Bauer, C. L. Mutel, and K. Volkart, "Life Cycle Assessment of Power-to-Gas: Approaches, system variations and their environmental implications," *Appl Energ*, vol. 190, pp. 326-338, 2017.
[30] A. Mayyas and M. Mann, "Manufacturing competitiveness analysis for hydrogen refueling stations," *International Journal of Hydrogen Energy*, vol. 44, no. 18, pp. 9121-9142, 2019.
[31] Y. Zhang, P. E. Campana, A. Lundblad, and J. Yan, "Comparative study of hydrogen storage and battery storage in grid connected photovoltaic system: Storage sizing and rule-based operation," *Appl Energ*, vol. 201, pp. 397-411, 2017.
[32] I. S. Steel, "CO2: Facts and Scientific Observations," *Availabe online: https://www. worldstainless. org/Files/issf/non-imagefiles/PDF/ISSF_Stainless_Steel_and_CO2. pdf (accessed on 2021-01-10)*, 2015.
[33] S. Niaz, T. Manzoor, and A. H. Pandith, "Hydrogen storage: Materials, methods and perspectives," *Renewable and Sustainable Energy Reviews*, vol. 50, pp. 457-469, 2015.
[34] W. K. Biswas, V. Duong, P. Frey, and M. N. Islam, "A comparison of repaired, remanufactured and new compressors used in Western Australian small-and medium-sized enterprises in terms of global warming," *Journal of Remanufacturing*, vol. 3, no. 1, pp. 1-7, 2013.
[35] R. Fu, D. J. Feldman, and R. M. Margolis, "US solar photovoltaic system cost benchmark: Q1 2018," National Renewable Energy Lab.(NREL), Golden, CO (United States), 2018.
[36] A. Wang, K. v. d. Leun, D. Peters, and M. Buseman, "European Hydrogen Backbone: How a dedicated hydrogen infrastructure can be created july 2020," 2020.
[37] Statista. " Forecast capital expenditure of a conventional natural gas combined-cycle power plant in the United States from 2022 to 2050 " https://www.statista.com/statistics/243707/capital-costs-of-a-typical-us-combined-cycle-power-plant/ (accessed.
[38] B. Tranberg, L. J. Schwenk-Nebbe, M. Schäfer, J. Hörsch, and M. Greiner, "Flow-based nodal cost allocation in a heterogeneous highly renewable European electricity network," *Energy*, vol. 150, pp. 122-133, 2018/05/01/ 2018, doi: https://doi.org/10.1016/j.energy.2018.02.129.

[39] J. Ikäheimo, J. Kiviluoma, R. Weiss, and H. Holttinen, "Power-to-ammonia in future North European 100 % renewable power and heat system," *International Journal of Hydrogen Energy*, vol. 43, no. 36, pp. 17295-17308, 2018, doi: 10.1016/j.ijhydene.2018.06.121.
[40] P. L. S. M. K. Mann, "Life Cycle Assessment of a Natural Gas Combined-Cycle Power Generation System," NREL, 2000.
[41] C. Smith, A. K. Hill, and L. Torrente-Murciano, "Current and future role of Haber–Bosch ammonia in a carbon-free energy landscape," *Energy & Environmental Science*, vol. 13, no. 2, pp. 331-344, 2020, doi: 10.1039/c9ee02873k.
[42] R. Nayak-Luke, C. Forbes, Z. Cesaro, R. Bañares-Alcántara, and K. H. R. Rouwenhorst, "Techno-Economic Aspects of Production, Storage and Distribution of Ammonia," *Techno-Economic Challenges of Green Ammonia as Energy Vector; Bañares-Alcántara, R., Valera-Medina, A., Eds*, pp. 191-208, 2020.
[43] R. M. Nayak-Luke and R. Bañares-Alcántara, "Techno-economic viability of islanded green ammonia as a carbon-free energy vector and as a substitute for conventional production," *Energy & Environmental Science*, vol. 13, no. 9, pp. 2957-2966, 2020, doi: 10.1039/d0ee01707h.
[44] T. Media. "Historic inflation Belgium - CPI inflation." https://www.inflation.eu/en/inflation-rates/belgium/historic-inflation/cpi-inflation-belgium.aspx (accessed.
[45] D. Coppitters, "Robust design optimization of hybrid renewable energy systems," Ph.D., Mechanical Engineering, University of Mons & Vrije Universiteit Brussel, 2021.
[46] A. Simons and C. Bauer, "Life cycle assessment of hydrogen production," in *Transition to Hydrogen: Pathways toward Clean Transportation*, A. Wokaun and E. Wilhelm Eds. Cambridge: Cambridge University Press, 2011, pp. 13-57.
[47] H. I. Coalition, "<20 05 10 Hydrogen Import Coalition.pdf>," 2021. [Online]. Available: https://www.portofantwerp.com/sites/default/files/Hydrogen%20Import%20Coalition.pdf
[48] E. Asen. "Carbon Taxes in Europe." https://taxfoundation.org/carbon-taxes-in-europe-2019/ (accessed.
[49] DNV. " Solar PV powering through to 2030 " https://www.dnv.com/to2030/technology/solar-pv-powering-through-to-2030.html (accessed.
[50] statista. "Average monthly electricity wholesale prices in selected countries in the European Union (EU) from January 2020 to December 2022 " https://www.statista.com/statistics/1267500/eu-monthly-wholesale-electricity-price-country/ (accessed.
[51] 2021. "Levelized Cost Of Energy, Levelized Cost Of Storage, and Levelized Cost Of Hydrogen." https://www.lazard.com/perspective/levelized-cost-of-energy-levelized-cost-of-storage-and-levelized-cost-of-hydrogen/ (accessed.

[52] M. W. Mkaouer and M. Kessentini, "Chapter Four - Model Transformation Using Multiobjective Optimization," in *Advances in Computers*, vol. 92, A. Hurson Ed.: Elsevier, 2014, pp. 161-202.

[53] M. Stein, "Large Sample Properties of Simulations Using Latin Hypercube Sampling," *Technometrics*, vol. 29, no. 2, 1987, doi: 10.2307/1269769.

[54] S. Ghoreishi, A. Clausen, and B. Joergensen, " Termination Criteria in Evolutionary Algorithms: A Survey," *JO - Proceedings of the 9th International Joint Conference on Computational Intelligence - IJCCI*,, 2017, doi: 10.5220/0006577903730384.

[55] U. Lee, S. Park, and I. Lee, "Robust design optimization (RDO) of thermoelectric generator system using non-dominated sorting genetic algorithm II (NSGA-II)," *Energy*, vol. 196, 2020, doi: 10.1016/j.energy.2020.117090.

6 Annex: Optimisation algorithm and modelling approaches

In this work, the computational framework, namely RHEIA [4] is used to facilitate multi-objective optimisation of the engineering model and uncertainty quantifications. The framework is based on Python programming language and the engineering models. The well-established evolutionary algorithm Non-dominated Sorting Genetic Algorithm (NSGA-II) is used for the deterministic design optimisation process. The NSGA-II is used to optimise (maximise, minimise) the quantity of interest so called design variable. The ***design variable*** _for instance levelized cost of energy (LCOE), quantity of produced H2 (m_H2), and/or global warming potential (GWP)_ can be changed by the designer to achieve the optimal values. In contrast, the ***model parameters*** are beyond the designer's control. For instance, the solar radiation and temperature over 6780 hours annually cannot be controlled by the designer, the capital expenditure (CAPEX) and the operating expenditure (OPEX).

6.1 Installing RHEIA framework and required packages

First, Python can be installed in several ways. If the distribution platform is no constraint, we recommend installing Python via the Anaconda Python distribution, which includes many common packages in data science (and used in RHEIA), such as NumPy and SciPy [4]. Package dependencies. Several packages are required to run RHEIA to evaluate the hydrogen-based energy system models:

- Included in Anaconda native installation:
  - NumPy
  - SciPy
- Other packages:
  - pyDOE
  - SobolSequence

To perform deterministic design optimisation:

- Included in Anaconda native installation:
  - NumPy
- Other packages:
  - pyDOE

- DEAP

To perform robust design optimisation:

- Included in Anaconda native installation:
  - NumPy
  - SciPy
- Other packages:
  - pyDOE
  - SobolSequence
  - DEAP

The framework can be installed on C:\ drive as follows C:\Users\user.name\Anaconda3\Lib\site-packages\rheia. In the framework folder, the following sub-folders are organized: CASES, OPT, POST_PROCESSING, RESULTS and UQ.

RHEIA

+---CASES

+---OPT

+---POST_PROCESS

+---RESULTS

+---UQ

In the following section, the modelling tool, structure, folders and files will be explained in details.

6.2 Modelling tool, Structure, folders and files

Figure 16 illustrates the optimisation process where the genetic algorithm functions is in the outer loop and the polynomial chaos expansion algorithm is in the inner loop (Figure 16).

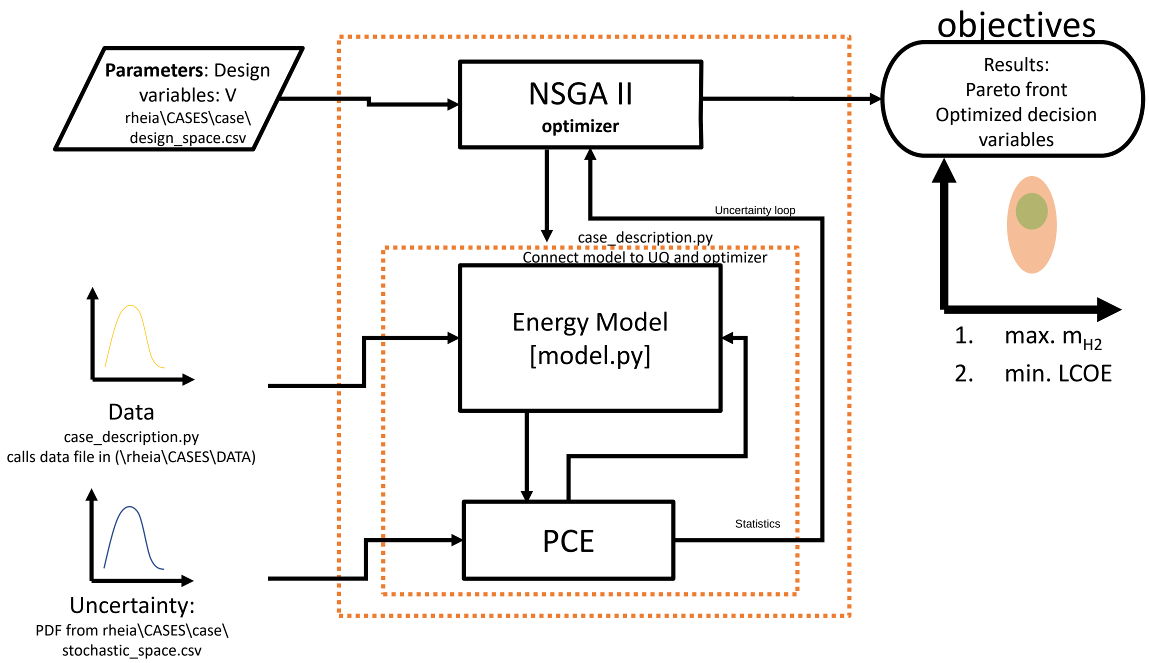

Figure 16 Flow diagram of the optimisation process where the genetic algorithm functions is in the outer loop and the polynomial chaos expansion algorithm is in the inner loop.

In the outer loop, the iteration of the NSGA-II procedure starts with an offspring Q_t which is created from the population P_t (Figure 17, 1) using genetic operators such as crossover and mutation [52]. From the population and offspring, the design samples are sorted [53] in non-dominated fronts, based on their dominance in the objectives (Figure 17, 2). From the first front F_1, design samples are all stored in the new population P_{t+1} (Figure 17, 3). in the second front F_2, the design samples are sorted based on crowding distance (Figure 17, 4) and the remaining places in the new population P_{t+1} are filled with the design samples with the highest crowding distance among the samples in F_2 (Figure 17, 5). The remaining design samples in F2 and F3 are rejected [45].

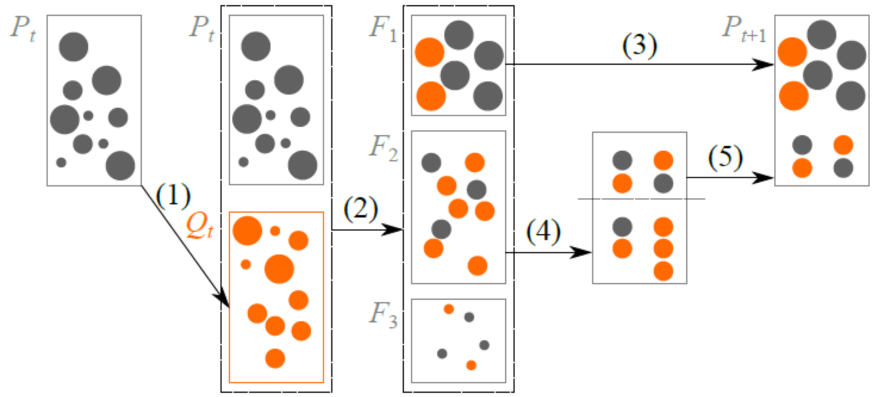

Figure 17 The main procedure of the evolutionary algorithm Nondominated Sorting Genetic Algorithm (NSGA-II) [45]

The number of iterations for (NSGA-II) process depends on the stopping criterion. Either direct termination criteria or performance indicator termination criteria can be used. The direct termination criteria (e.g., limiting the time budget, stop when the difference between the best objective value and the mean of the objective values in the last generation is below a threshold). In the performance indicator termination criteria (e.g., the hyper-volume metric, which represents the volume defined by the set of design values and a reference sample in the objective space, Figure 2.4) [54]. The Robust design optimisation (RDO) using NSGA-II procedure is explained in details by [45, 55].

The **polynomial chaos expansion (PCE)** (Figure 16) is used for robust design optimisation and uncertainty quantification. The loop is initiated by a dictionary (Code 1) and each design sample undergoes an uncertainty quantification analysis. The analysis determines the mean and standard deviation on the quantity of interest for that design sample by propagating the uncertain parameters. The mean and standard deviation for each quantity of interest from each design sample set are returned to the genetic algorithm. The best-performing design samples are stored, and new design samples are generated, for which the mean and standard deviation on the quantity of interest are quantified again in the inner loop. This process is repeated until meeting the stopping criterion, which evaluates these results and proceeds to generate new designs that need to be evaluated in the uncertainty loop.

6.2.1 Folder and files

In RHEIA **work-package folder**, the CASES folder includes pre-modelled cases as examples. In each case folder, files are required to characterise and evaluate the case. In the following, an e.g. for the H2_FUEL case:

```
RHEIA
+---CASES
|       +---H2_FUEL
|       |       | case_description.py
|       |       | h2_fuel.py
|       |       | design_space
|       |       | stochastic_space
|       |       | __init__.py
```

To run a model, either the system model is present (Python-based model, e.g. h2_fuel.py), or a Python wrapper is present, which is called by e.g., a closed-source executable file. The *design_space* file includes the bounds for the design variables and the mean values for the model parameters. The *stochastic_space* file includes the stochastic characterization of the random parameters (i.e., the variance and distribution type). Finally, the *case_description* Python module operates as a Python wrapper, which contains a function to read and store the fixed parameters for model evaluation and a function to evaluate the system model. It enables the evaluation of the system model with the samples provided by the optimisation or uncertainty quantification algorithms [4, 45].

Initiating the procedure: the optimisation procedure can be started by characterizing a *dictionary* and providing this dictionary as an argument to the *run_opt()* function. For instance, the following dictionary (Code 1) with the input sample names (as defined in *design_space.csv* and *stochastic_space.csv*). The corresponding values are the values generated by the optimisation or uncertainty quantification algorithm. The dictionary passes values directly as an argument to the model for evaluation.

The *case_description* module enables to connect the system model to the uncertainty quantification and optimisation algorithms. The module includes two functions: *set_params()* and *evaluate()*.

```
# dictionary
import rheia.OPT.optimisation as rheia_opt
import multiprocessing as mp

dict_opt = {'case':                    'H2_FUEL_CO2',
            'objectives':              {'ROB': (-1, -1)},#(-mu, -std)
            'stop':                    ('BUDGET', 72000),
            'n jobs':                  int(mp.cpu_count() / 2),
            'population size':         20,
            'results dir':             'run_1',
            'pol order':               2,
            'objective names':         ['LCOH', 'CO2'],
            'objective of interest':   ['LCOH'],
            }

if __name__ == '__main__':
    rheia_opt.run_opt(dict_opt)
```

Code 1 optimisation dictionary to perform a deterministic design optimisation

Results folder: the results of deterministic, robust optimisation and uncertainty quantification of each case can be found in the results folder (e.g. C:\Users\username\Anaconda3\Lib\site-packages\rheia\RESULTS).

```
+---RESULTS
|       +---H2_FUEL_CO2
|       |       +---ROB
|       |       |       \---run_1
|       |       |       |       |fitness
|       |       |       |       |population
|       |       |       |       |STATUS
```

The results can be plotted using the methods provided in the post-processing classes, defined in the post-processing module (Code 3).

RHEIA

+---POST_PROCESS

| | lib_post_process.py

| | __init__.py

6.3 Methodology for the deterministic optimisation

The system model output of interest is a deterministic design optimisation technique optimised by searching a finite design space constructed by selected model input parameters (also called design variables). Robust design optimisation works on the same principle. Fundamental changes focus on the probabilistic treatment of model input parameters (i.e. uncertainty definition and propagation). This determines the optimisation of the mean and the minimization of the standard deviation of the considered model outputs. The multi-objective optimisation algorithm used in RHEIA is the Nondominating Sorting Genetic Algorithm (NSGA-II). The design variables and model parameters are characterized in the *design_space.csv* file. As per robust design optimisation, the uncertainty on the respective design variables and model parameters is characterized in the *stochastic_space.csv* file. The system model evaluations are coupled with the optimisation algorithm in *case_description*.

6.3.1 Run deterministic design optimisation in RHEIA frame work

To perform a deterministic design optimisation, the following optimisation dictionary has to be filled and passed as an argument to the *run_opt()* function, see the following Code 2.

```
import rheia.OPT.optimisation as rheia_opt
import multiprocessing as mp

dict_opt = {'case':                    'H2_FUEL_CO2',
```

```
             'objectives':             {'DET': (-1, -1)},
             'stop':                   ('BUDGET', 2000),
             'n jobs':                 int(mp.cpu_count() / 2),
             'population size':        20,
             'results dir':            'run_1',
             }

if __name__ == '__main__':
    rheia_opt.run_opt(dict_opt)
```

Code 2 optimisation dictionary to perform a deterministic design optimisation

For instance, in the dictionary, the case folder name 'H2_FUEL_CO2' is provided, followed by the optimisation type 'DET' and the weights for both objectives, i.e. minimization for the first returned objective LCOH and minimise for the second returned objective IC (CO_2 emissions). The objectives LCOH and IC (CO_2 emissions) are stated in the *case_description.py* and the optimisation results are stored in the directory as it is set in the optimisation dictionary (Code 2).

The results can be plotted using the methods provided in the post-processing classes, defined in the post-processing module. For instance, Code 3 is used to post-process data, y[0] and y[1] refer to the optimised objectives, e.g. LCOE and IC (CO_2 emissions). (x_in in x) refers to the design parameters e.g. (n_pv) PV capacity range, (n_PEMEL) electrolyser capacity range which are stated in the *design_space* file in the CASE folder. (additional information is available on the framework website).

```
# -*- coding: utf-8 -*-
"""
Created on Thu Jun  2 20:30:25 2022

@author: zayoud
"""

import rheia.POST_PROCESS.post_process as rheia_pp
import matplotlib.pyplot as plt

case = 'H2_FUEL_CO2'
eval_type = 'DET'
my_opt_plot = rheia_pp.PostProcessOpt(case, eval_type)
result_dir = 'climate_Midelt_ma_co2'

y, x = my_opt_plot.get_fitness_population(result_dir)

plt.plot(y[0], y[1], '-o')
plt.xlabel('LCOE [euro/kg]')
plt.ylabel('ci [kg.CO2_eq/kg.H2]')
plt.show()

for x_in in x:
    plt.plot(y[0], x_in, '-o')
```

```
plt.legend(['pv capacity'])
plt.xlabel('LCOE [euro/kg]')
plt.ylabel('capacity [kW]')
plt.show()
```

Code 3 Postprocessing the performed deterministic design optimisation and plotting the results

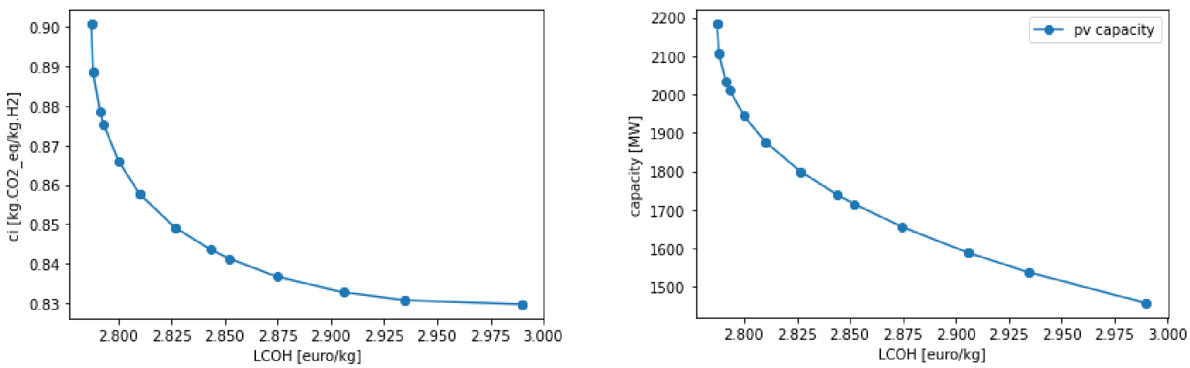

Figure 18 (LHS) Pareto front of the optimisation objectives shows the trad-off between LCOH and CI (CO2 emissions intensity); (RHS) the design variable versus optimisation objective LCOH

6.3.2 Uncertainty characterisation: Polynomial Chaos Expansion (PCE)

Polynomial Chaos Expansion (PCE) is adopted as an uncertainty quantification (UQ) method (Figure 17). Since PCE provides significant advantages, such as the analytical quantification of the statistical moments and the sensitivity indices (i.e., Sobol' indices). The PCE is linked with NSGA-II optimiser in the RHEIA framework [4].

Uncertainty can be divided into two categories: epistemic uncertainty, which is due to a lack of knowledge about a certain parameter, and aleatory uncertainty, which is related to the unknown evolution of a parameter value. The RHEIA framework is used to optimise and quantify this uncertainty, particularly in renewable energy systems. It has been successfully applied in various scenarios involving photovoltaic systems, micro gas turbines, wind turbines, and ammonia synthesis plants.

6.3.2.1 Determination of the polynomial order

According to the PCE truncation scheme, the number of model evaluations needed to create a PCE for each design sample depends on the maximum polynomial degree. For a maximum polynomial degree of 1, 2, and 3, the number of model evaluations required is 26, 182, and 910, respectively. The optimal polynomial degree for an accurate expansion must be determined iteratively, and more information on this process can be found in the section on design space screening.

```
import rheia.UQ.uncertainty_quantification as rheia_uq
import multiprocessing as mp
case = 'H2_FUEL'
n_des_var = 20
var_dict = rheia_uq.get_design_variables(case)
X = rheia_uq.set_design_samples(var_dict, n_des_var)
for iteration, x in enumerate(X):
    rheia_uq.write_design_space(case, iteration, var_dict, x, ds =
'design_space_tutorial.csv')
    dict_uq = {'case':                   case,
               'n jobs':                 int(mp.cpu_count()/2),
               'pol order':              1,
               'objective names':        ['LCOH','mh2'],
               'objective of interest': 'LCOH',
               'results dir':            'sample_tutorial_%i' %iteration
               }
    if __name__ == '__main__':
        rheia_uq.run_uq(dict_uq, design_space =
'design_space_tutorial_%i.csv' %iteration
```

Code 4 Determination of the polynomial order for specific case e.g. case = 'H2_FUEL' and objective of interest e.g. LCOH

The functions *get_design_variables()* and *set_design_samples()* are used to generate the samples through Latin Hypercube Sampling and to assemble the bounds of the design variables and, respectively. Then, *design_space.csv* files are created through *write_design_space()* – one for each design sample – and a PCE is constructed for each sample. The process is repeated for 'pol order': 1, 2 and 3.

To determine the worst-case LOO error for the 20 design samples, a *post_process_uq* class object is instantiated, followed by the call of the *get_loo()* method (Code 5).

```
import rheia.POST_PROCESS.post_process as rheia_pp

case = 'H2_FUEL'
pol_order = 1
my_post_process_uq = rheia_pp.PostProcessUQ(case, pol_order)
result_dirs = ['sample_tutorial_%i' %i for i in range(20)]

objective = 'LCOH'

loo = [0]*20
for index, result_dir in enumerate(result_dirs):
```

```
    loo[index] = my_post_process_uq.get_loo(result_dir, objective)

print(max(loo))
```

Code 5 determine the worst-case LOO error for the 20 design samples, a post_process_uq class object is instantiated, followed by the call of the get_loo() method

For the provided design samples with a maximum polynomial degree of 1, the worst-case leave-one-out error is 0.0701. This error decreases to 0.0140 when the maximum polynomial degree is increased to 2. For this tutorial, a maximum polynomial degree of 2 is considered acceptable and is therefore chosen for the PCE truncation scheme in the robust design optimisation process.

6.3.2.2 Reducing the stochastic dimension

The Sobol' index is a statistical measure that is used to quantify the importance of a particular variable or factors in the variability of a system. It is commonly used in sensitivity analysis to identify the variables that have the greatest impact on the output of a model. The Sobol' indices can be used to analyze the 20 samples generated to determine the polynomial order. These indices allow for the identification of the stochastic parameters that have a minimal impact on the standard deviation of the system. These parameters can be treated as deterministic with little effect on the accuracy of the mean and standard deviation in the robust design optimisation process. More information on this method can be found in the section on design space screening. For a polynomial order of 2, the following parameters can be identified as having a negligible Sobol' index.

```
import rheia.POST_PROCESS.post_process as rheia_pp
case = 'H2_FUEL'
pol_order = 2
my_post_process_uq = rheia_pp.PostProcessUQ(case, pol_order)
result_dirs = ['sample_tutorial_%i' %i for i in range(20)]
objective = 'LCOH'

my_post_process_uq.get_max_sobol(result_dirs, objective, threshold=1./12.)
```

Code 6 determine the worst-case LOO error for the 20 design samples, a post_process_uq class object

A threshold for the Sobol' index is set at 1/12 (1 divided by the number of uncertain parameters).

Out of the 12 uncertain parameters, 5 have a maximum Sobol' index below this threshold, meaning that they can be treated as deterministic without significantly affecting the calculated statistical moments of the LCOH. This reduction in the number of uncertain parameters results in a 60% decrease in computational cost, as only 72 model evaluations are needed to construct a PCE for the remaining 7 uncertain parameters, compared to the 182 model evaluations required for all 12 uncertain parameters. By following this strategy, the 5 parameters with a minimal contribution can be removed from the "*stochastic_space.csv*" file.

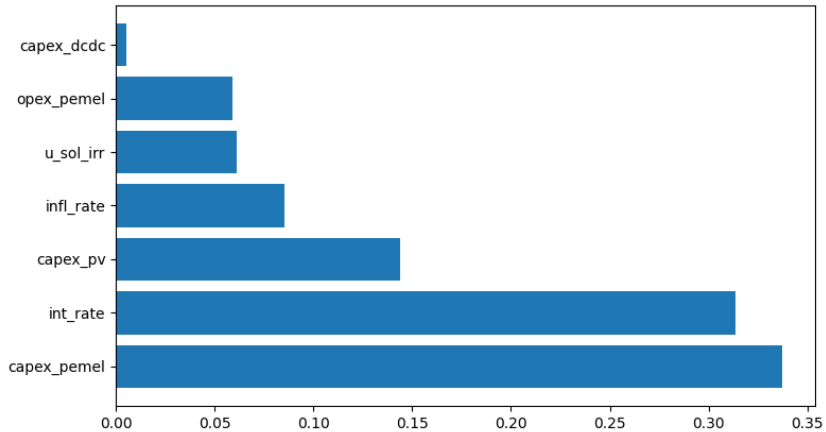

Figure 19 Sobol' indices illustrate that the uncertainty on the interest rate and the investment cost of the PV array and electrolyser stack dominate the uncertainty on the LCOH.

Finally, the probability density function is plotted with the *get_pdf()* method:

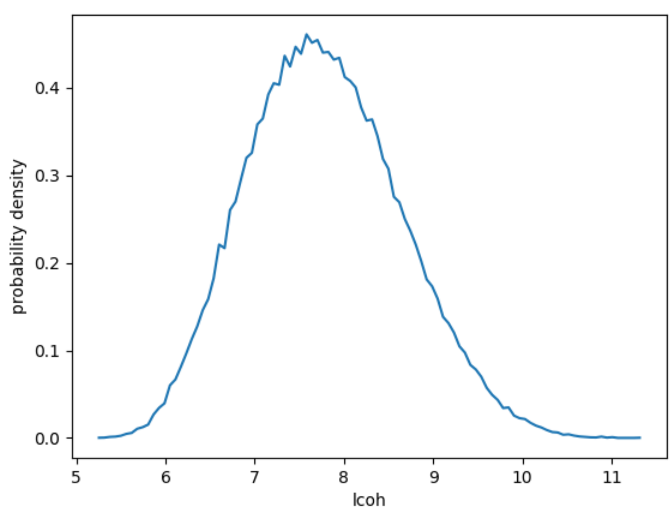

Figure 20 The probability density function of LCOE

The procedure of uncertainty quantification can be performed for variety of objective of interest. However, the $CAPEX_{PEMEL}$, $CAPEX_{PV}$, interest rate and $OPEX_{PEMEL}$ have a high Sobol' indices and can be considered uncertain in the planning stage, but are fixed during system operation.